Boson localization and excitations of liquid ^{4}He confined in gelsil

Francesco Albergamo,[1] Jacques Bossy,[2] Jonathan V. Pearce,[3,4] Helmut Schober,[3] and Henry R. Glyde[4]
[1]*European Synchrotron Radiation Facility, Boîte Postale 220, F-38043 Grenoble Cedex, France*
[2]*Centre de Recherche sur les Très Basses Températures, CNRS, BP 166, 38042 Grenoble Cedex 9, France*
[3]*Institut Laue-Langevin, BP 156, 38042 Grenoble, France*
[4]*Department of Physics and Astronomy, University of Delaware, Newark, Delaware 19716-2570, USA*
(Received 20 December 2006; revised manuscript received 17 May 2007; published 6 August 2007)

We present neutron scattering measurements of the phonon-roton (P-R) modes of liquid ^{4}He at saturated vapor pressure confined in 44 Å mean pore diameter gelsil in the wave vector range $0.4 \leqslant Q \leqslant 2.15$ Å^{-1}. Layer modes, modes which propagate in the liquid layers adjacent to the porous media walls, were also observed at wave vectors in the roton region ($Q \simeq 1.95$ Å^{-1}) but not at $Q \lesssim 1.7$ Å^{-1}. The first goal is to document the filling dependence of the dynamic response and of the P-R mode energies and widths more systematically than has been done in the past. As the gelsil is filled with ^{4}He, the P-R and layer modes are first observed at a fractional filling of $f=76\%$ at low temperature ($T=0.4$ K). At fillings $f=76\%$, the P-R mode energies lie below the bulk superfluid ^{4}He values in the wave vector range $0.4 \leqslant Q \leqslant 1.7$ Å^{-1}, especially at $Q \simeq 1.1$ Å^{-1}, as observed in helium films. As filling is increased, the intensity in the P-R mode increases markedly and the P-R mode energies move toward bulk superfluid values taking bulk values at full filling. The second goal is to determine the temperature dependence of the intensity in the P-R modes in a media in which the superfluid-normal transition temperature $T_c=1.92$ K is independently known and lies well below the bulk liquid value $T_\lambda=2.17$ K. As temperature is increased, the intensity in the P-R and layer modes decreases. However, a well-defined P-R mode is observed at temperatures up to $T \simeq 2.15$ K, above $T_c=1.92$ K. Since well-defined modes exist because there is Bose-Einstein condensation (BEC), this suggests that there is BEC above T_c, probably localized. Localized BEC appears to exist up to $T \simeq T_\lambda$.

DOI: 10.1103/PhysRevB.76.064503 PACS number(s): 67.40.Db, 61.12.Ex

I. INTRODUCTION

Liquid ^{4}He confined in porous media[1] is a simple example of bosons in disorder.[2–8] Other examples are Cooper pairs (bosons) in high T_c superconductors[9,10] or in disordered thin films,[11] Josephson junction arrays,[12] flux lines in dirty superconductors,[13] and atoms in disorder in optical traps.[14] Superfluidity of liquid ^{4}He in porous media has been investigated for over 50 years.[1] A goal in the study of superfluidity has been to determine how much the normal to superfluid transition temperature T_c is suppressed below the bulk value, T_λ, by confinement and disorder and how the critical exponents governing the superfluid density, $\rho_s(T)$, are modified and to make comparisons with predictions. In contrast, measurement of the excitations of liquid ^{4}He in porous media has only recently begun.[7,15–24] Of equal interest is to determine how Bose-Einstein condensation (BEC) and the elementary excitations are modified by disorder and to make the connection between these changes and the changes in superfluid behavior.

In this paper, we report neutron scattering measurements of the fundamental phonon-roton (P-R) excitations of superfluid ^{4}He at saturated vapor pressure (SVP) in a gelsil glass having 44 Å mean pore diameter (mpd). The first goal is to determine the temperature dependence of the phonon-roton modes. Particularly, the aim is to determine the temperature at which well-defined P-R modes cease to be observed and compare this temperature with T_c and T_λ. The present gelsil was selected because the pore size is small enough[24,25] that the normal-superfluid transition temperature in it, $T_c=1.92$ K at SVP, is suppressed significantly below the bulk value, $T_\lambda=2.172$ K at SVP, so that there is a clear difference between T_c and T_λ. Thus, whether well-defined modes disappear at T_c or T_λ can be distinguished. The T_c was determined from changes in the ultrasound velocity and attenuation at the superfluid to normal transition.[24,25] The phase diagram of helium in the present 44 Å gelsil appears in Fig. 1 of Ref. 24 showing T_c ranging from 1.92 K at SVP to 1.35 K at $p=35$ bars. At SVP, T_c in the present gelsil lies between T_c in Vycor[1,34,35] ($T_c=1.95$ and 2.05 K) (70 Å mpd) and $T_c \simeq 1.3$ K in 25 Å mpd gelsil.[66] Comparison will also be made with the P-R modes under pressure in the same sample.[24]

A second goal is to document the filling dependence of the excitations. The pore size of 44 Å is still large enough that, at or near full filling, approximately 50% of the ^{4}He in the media is liquid; the remainder is solid near the pore walls. Thus, there is liquid over a wide enough filling range to investigate the filling dependence of the P-R modes. Also, the pore size (44 Å) is close to the pore diameter of an MCM-41 sample (47 Å) in which we have observed liquid ^{4}He at negative pressures.[22]

In all porous media investigated to date, superfluid ^{4}He at SVP supports well-defined P-R excitations.[7,20,23] At full filling, the mode energies are the same as in the bulk, both at low temperature and as a function of temperature. Within precision, the mode lifetimes are also the same. Up to pressures of 25 bars and at low temperature, the mode energies are also the same as in the bulk within precision.[24] At $p \geqslant 25$ bars, the P-R mode at wave vectors Q in maxon region, $Q \simeq 1.1$ Å^{-1}, broadens markedly and becomes unobservable.[24] This can be understood since at higher pres-

sure, the P-R mode energy in the maxon region exceeds twice the roton energy (2Δ) and the mode can decay into two rotons. At still higher pressure, all the modes disappear including the roton.[24] In porous media, liquid ^{4}He also supports a layer mode, a mode propagating in the liquid layers adjacent to the media walls.[16–21] This is the layer mode that was first observed in superfluid helium films on graphite.[26–29] In porous media, the layer mode is usually observed at wave vectors in the roton region only.

In bulk liquid ^{4}He, as temperature is increased, well-defined P-R modes, BEC, and superfluidity all disappear at the same temperature, the superfluid-normal transition temperature T_λ. The P-R modes in superfluid ^{4}He are uniquely well defined with long lifetimes (e.g., at 1 K) because there is a condensate and no available decay channels for the mode. This is the case at all pressures from SVP up to 25.3 bars where the superfluid solidifies.[30–33] In all porous media investigated, the normal-superfluid transition temperature T_c is suppressed below T_λ.[1,34,35] In contrast to the bulk, we have observed well-defined P-R modes above T_c (in the normal phase) in Vycor[19,23] and 25 Å gelsil.[36] This suggests that there is BEC above T_c in porous media,[7,19,23,36] at temperatures $T_c < T < T_\lambda$. A goal here is to investigate this effect in a porous media in which T_c lies well below T_λ ($T_c = 1.92$ K versus $T_\lambda = 2.172$ K at SVP) and in which the neutron scattering intensity from P-R modes is three times larger than that in Vycor.

II. EXPERIMENT

A. Porous media sample

The porous silica glass sample[37] was prepared specifically for the present and previous[24,25] measurements by 4F International Co.[38] using a sol-gel technique. The pores have an irregular shape in an interconnected structure. To characterize the gelsil, 4F International conducted N_2 adsorption isotherm measurements which are reproduced in Fig. 1. These isotherms were analyzed by 4F International using the BJH model of Barrett *et al.*,[39] which revealed a 44 Å mean pore diameter and an approximately Gaussian pore diameter distribution with a half width at half maximum of 20 Å. The BET surface area of Brunauer *et al.*[40] was determined to be 602 m^2/g with a porosity of 50%. The sample consisted of two cylindrical rods of 10 mm diameter and 20 mm height each. The total mass of the sample was 2.50 g. The sample was outgassed at 50 °C in a vacuum of 10^{-8} mbar for 3 days.

We conducted helium adsorption isotherms at 2.51 K which are also shown in Fig. 1. These isotherms show that helium is adsorbed in the gelsil at low vapor pressure up to a filling of approximately $f=50\%$. This is interpreted as adsorption of two tightly bound "dead" layers of helium on the media walls. The first layer is believed to be amorphous solid, while the second could be an amorphous solid or a tightly bound liquid. Thereafter, the pressure increases slowly with the amount adsorbed up to a filling of $f=85\%$. This is interpreted as formation of less tightly bound liquid layers, denoted the multilayer, on top of the dead layers. A capillary condensation hysteresis loop begins at $f=85\%$ and a reduced pressure of about $p=0.6$ involving 15% of the total amount of ^{4}He adsorbed. The gelsil is full ($f=100\%$) at $n_{ads}=30.0$ mmol g^{-1} of ^{4}He.

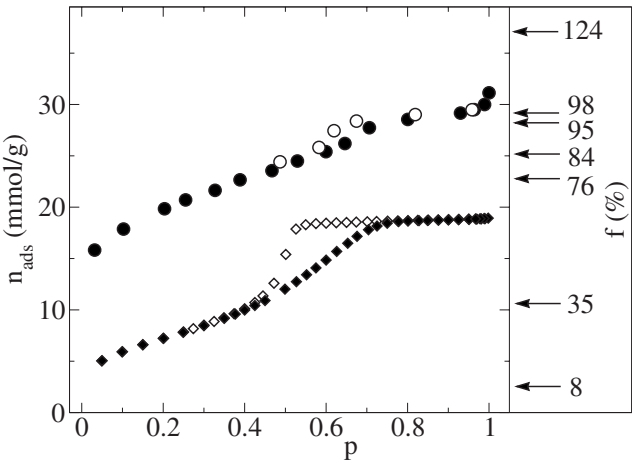

FIG. 1. Adsorption isotherms in the present porous gelsil sample. Diamonds are N_2 adsorption (solid) and desorption (open) isotherms at 77 K. Circles are helium adsorption (solid) and desorption (open) isotherms at 2.51 K. The amount adsorbed per gram of empty porous media versus the ratio of applied pressure to the saturated vapor pressure is shown. The arrows on the right hand side show the helium filling fractions (in %) at which neutron scattering measurements were performed.

B. Neutron scattering experiment

The inelastic neutron scattering measurements were performed on the IN6 spectrometer at the Institut Laue-Langevin, Grenoble, France. The incident neutron wavelength was $\lambda=4.62$ Å and the spectrometer resolution full width at half maximum was about 100 μeV. A ^{3}He cryostat was used to provide temperatures as low as 0.4 K. The temperatures and fillings at which data were taken are listed in Table I. At a temperature of $T=0.4$ K, the fillings ranged from 8% to 124%. At a filling of $f=95\%$, the temperature was varied from 0.4 to 2.25 K. At $f=124\%$, the sample is overfilled and some bulk liquid helium is condensed between the sample and the sample holder. This excess filling amounts to 7 mmol g^{-1} (equivalent to 17.5 mmol or 0.48 cm^3 of bulk liquid ^{4}He) at SVP. Data were collected in 337 ^{3}He detectors and rearranged in Q bins of width 0.05 $Å^{-1}$. The detection efficiencies were normalized using the scattered intensity from a vanadium standard.

III. DATA REDUCTION

Our goal is to determine the net inelastic scattering intensity from the excitations supported by the liquid in the gelsil pores. From the ^{4}He absorption isotherms shown in Fig. 1 and the discussion in the Introduction, we see that the ^{4}He is deposited in the gelsil as tightly bound layers on the gelsil walls for fillings up to $f=50\%$. We do not expect these tightly bound or dead layers to support excitations. We therefore take a filling between zero and 50% as our background

TABLE I. Temperature and fillings of the sample at which neutron scattering measurements were made. Typical errors on the temperature T and the amount of ^{4}He adsorbed in the gelsil, n_{ads}, are 0.01 K and 0.05 mmol g^{-1}, respectively.

T (K)	n_{ads} (mmol g^{-1})	Filling fraction (%)
0.40	2.41	8
3.30	10.54	35
0.40	22.71	76
0.40	25.12	84
0.40	29.39	98
0.40	28.77	95
1.35	28.72	95
1.45	28.74	95
1.60	28.71	95
1.70	28.68	95
1.80	28.65	95
1.90	28.60	95
2.00	28.55	95
2.25	28.37	95
0.40	37.11	124

or reference scattering intensity filling and present the data as net scattering relative to scattering at this filling. Examples of the total inelastic scattering intensity from helium plus gelsil are shown in Fig. 2 of Ref. 36. In this paper, we select the reference scattering intensity at $f=35\%$. A reference at some low filling (not zero) is useful since the bound layers on the gelsil reduce the small angle scattering from the irregular internal surfaces of the gelsil. There is then a smaller background arising from the gelsil itself. We present all the scattering intensities relative to that at $f=35\%$.

Examples of the net intensity $I(Q,\omega;T)$ at $Q=1.95$ Å^{-1} and $T=0.40$ K at several fillings are shown in Fig. 2. In Fig. 3, we show $I(Q,\omega;T)$ at $Q=1.95$ Å^{-1} and several temperatures at a constant filling of $f=95\%$. This net intensity $I(Q,\omega;T)$ consists predominantly of three components: a broad component $S_B(Q,\omega;T)$, a "singular component" $S_1(Q,\omega;T)$, describing the P-R and layer modes, and a multiple scattering intensity $I_{MS}(\omega;T)$, which is mainly due to elastic scattering from the MCM-41 plus inelastic scattering from a P-R excitation,

$$I(Q,\omega;T) = S_B(Q,\omega;T) + S_1(Q,\omega;T) + I_{MS}(\omega;T). \quad (1)$$

The sum of $S_B(Q,\omega;T)$ and $S_1(Q,\omega;T)$ is proportional to the dynamic structure factor $S(Q,\omega;T)$. The broad component $S_B(Q,\omega;T)$ depends on Q and T but is largely independent of filling for $f \geqslant 76\%$. It is therefore unlikely to originate from multiphonon scattering since the single excitation intensity varies greatly with filling, for example, a factor of 5 between $f=76\%$ and $f=98\%$ (see Fig. 2). At the lowest temperature, $T=0.4$ K, we attribute $S_B(Q,\omega;T)$ to scattering from the liquid helium layers closest to the gelsil walls. At higher temperature, a contribution to the broad component also arises from the scattering from all of the liquid helium, as already observed in previous studies of bulk[31,42] and confined[22] helium.

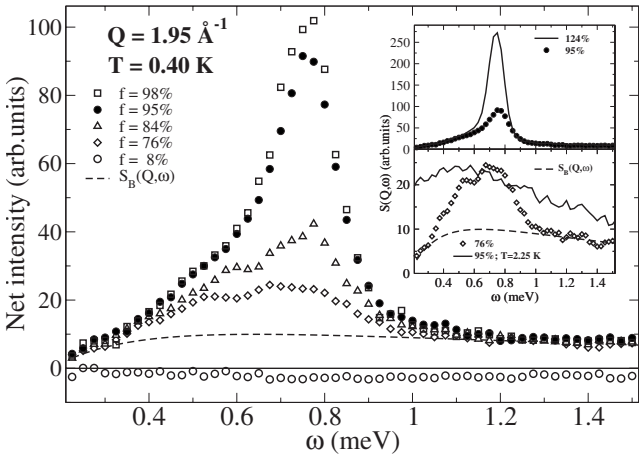

FIG. 2. Net scattering intensity $I(Q,\omega;T)$ from helium in gelsil at $Q=1.95$ Å^{-1} at $T=0.4$ K and the fillings indicated relative to a filling $f=35\%$. At $f=8\%$, the net intensity is slightly negative relative to $f=35\%$. The $S_B(Q,\omega)$ is the broad component of $I(Q,\omega)$ observed at fillings $f>76\%$ and is attributed to helium layers bound to the gelsil walls (see Sec. IV). Top inset: $I(Q,\omega)$ at $f=95\%$ and $f=124\%$; a fully filled sample plus 7 mmol g^{-1} of bulk liquid between the gelsil sample and the sample holder. Bottom inset: $I(Q,\omega)$ at $f=76\%$ and $T=0.4$ K and $f=95\%$ and $T=2.25$ K.

The IN6 spectrometer energy resolution could be checked using the scattering intensity linewidth at the highest filling, $f=124\%$. At this filling, the intensity arises largely from the bulk liquid ^{4}He between the sample and the sample holder. At $T=0.4$ K, the width of the bulk superfluid P-R mode is negligible[41] and the observed width arises entirely from the spectrometer resolution. The instrument resolution found in this way was consistent with previous values.[32]

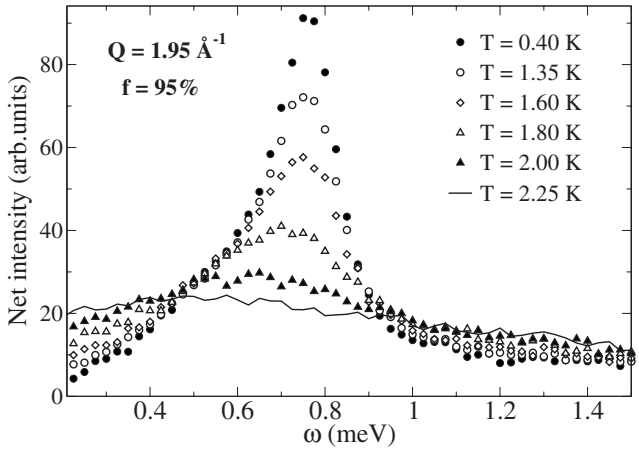

FIG. 3. Net scattering intensity $I(Q,\omega;T)$ from helium in gelsil at $Q=1.95$ Å^{-1} and filling $f=95\%$ relative to a filling of $f=35\%$ at several temperatures.

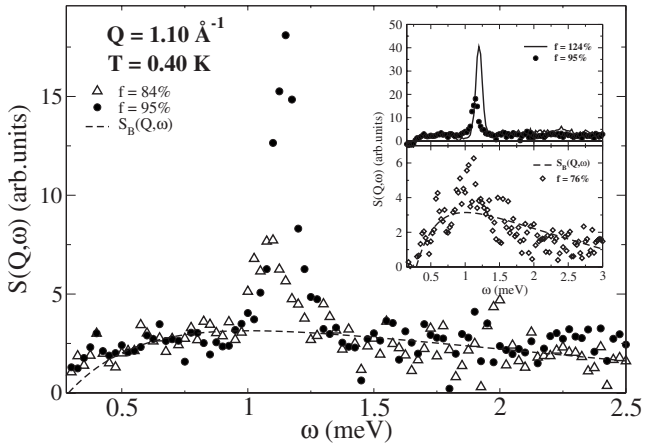

FIG. 4. The net dynamic structure factor, $S(Q,\omega)=S_1(Q,\omega)+S_B(Q,\omega)$, at $Q=1.10$ Å^{-1} of helium at $T=0.4$ K in gelsil at fillings $f=84\%$ and $f=95\%$. $S_B(Q,\omega)$ is the broad component. Top inset: $S(Q,\omega)$ at $f=95\%$ and $f=124\%$. Bottom inset: $S(Q,\omega)$ at $f=76\%$.

Multiple scattering determination and broad component

In general, multiple scattering can originate from a wide spectrum of scattering processes. However, since we present the net inelastic intensity from helium for fillings $f>35\%$ only, the net inelastic multiple scattering in the data must involve scattering from helium. In this event, $I_{\mathrm{MS}}(\omega,T)$ originates predominantly from inelastic scattering from a P-R mode (predominantly the roton) plus an elastic scattering from the silica. Essentially, when the neutron scatters elastically from the silica, the Q selection is lost. The roton, the most intense part of the P-R curve, therefore appears at all Q values. This contribution can be readily identified at the maxon wave vector, for example, since the maxon energy is much higher and well separated from the roton energy. The multiple scattering contribution is also approximately independent of Q. It can thus be identified from the signal which is not coming from $S_1(Q,\omega;T)$ or $S_B(Q,\omega;T)$ over the whole available Q range. Since $S_1(Q,\omega;T)$ is nonzero in a narrow ω interval, it can be safely taken out of the averaging procedure by just masking a reasonable window of ω. $I_{\mathrm{MS}}(\omega;T)$ broadens with temperature as the roton peak broadens.

The background component $S_B(Q,\omega;T)$ at $T=0.4$ K was represented by the function

$$F(Q,\omega)=k_Q+k'_Qe^{-\omega/\tau'_Q}-k''_Qe^{-\omega/\tau''_Q}, \tag{2}$$

where the five parameters, k_Q, k'_Q, τ'_Q, k''_Q, and τ''_Q, are free fitting parameters. Examples of this low temperature broad component are shown in Figs. 2 and 4 as a dashed line. At the highest temperature ($T=2.25$ K), the P-R peak is very broad or nonexistent. Indeed, as will be explained in Sec. IV C, the singular component $S_1(Q,\omega;T)$ is taken to be zero at $T=2.25$ K. As a result, the multiple scattering component involving P-R modes, $I_{\mathrm{MS}}(\omega;T)$, will also be zero at $T=2.25$ K. Thus, at $T=2.25$ K, Eq. (1) reduces to

$$I(Q,\omega;T)=S(Q,\omega;T=2.25\ \mathrm{K})=S_B(Q,\omega;T=2.25\ \mathrm{K}). \tag{3}$$

At intermediate temperatures, $S_B(Q,\omega;T)$ is expressed as a linear combination of the $T=0.4$ K and $T=2.25$ K limiting cases, as described in Sec. IV C.

To determine the multiple scattering $I_{\mathrm{MS}}(\omega;T)$, $S_B(Q,\omega;T)$ was subtracted from the data. $I_{\mathrm{MS}}(\omega;T)$, which is approximately independent of scattering angle, was evaluated by averaging the signal for different Q values at energies well separated from the P-R peak at each temperature and filling. The multiple scattering contribution is then permanently subtracted from all the spectra.

IV. ANALYSIS AND RESULTS

A. Qualitative features

A qualitative analysis of the data in Figs. 2 and 4 suggests the following:

(1) At fillings less than $f=35\%$, the scattering intensity is broad and does not contain a P-R mode. The intensity at the lowest filling, $f=8\%$, is lower but qualitatively the same as that at $f=35\%$ in the energy range investigated. Thus, the net scattering intensity for $f=8\%$ relative to a filling of $f=35\%$ is slightly negative (see Fig. 2). Up to $f=35\%$, the inelastic response is spread over a wide energy range.

(2) A three-dimensional (3D)-like P-R mode and a layer mode are first observed at a filling of $f=76\%$. For example, the net intensity at $f=76\%$ shown in Fig. 2 has a broad peak centered at $\omega\approx0.8$ meV for $Q=1.95$ Å^{-1} which we interpret as the first signs of a roton mode. The intensity also has a second broad peak at $\omega\approx0.5$ meV which we interpret as the first appearance of a layer mode. The intensity in these two modes grows rapidly with increasing filling. At $Q<1.80$ Å^{-1}, we observe only a P-R mode (no layer mode) as shown in Fig. 4. The filling $f=76\%$ lies below the apparent onset of capillary filling given by the lower limit of the hysteresis loop in the adsorption diagram (Fig. 1) which begins at $f=84\%$. This finding is in contrast to our finding in MCM-41 (Ref. 43) in which we found a correspondence between capillary condensation and the presence of a P-R mode signal. Observation of a P-R mode below $f=84\%$ suggests either that ^{4}He can capillary condense in the smallest pores at pressures below the hysteresis loop or that, at this filling, the liquid multilayer in the present gelsil is thick enough to support the P-R mode.

(3) The energy of the P-R excitations depends on filling, as shown in Fig. 4 and as observed for P-R modes in helium films[28,29] and in other porous media.[18,22,36,43] The filling dependence of the P-R energies is presented below in Fig. 6.

B. Filling dependence

The P-R mode and the layer mode (L) were investigated at four fillings, $f=76\%$, 84%, 95%, and 98%, at $T=0.4$ K. The contribution to the total net scattered intensity in Eq. (1) arising from the P-R and layer modes is denoted by $S_1(Q,\omega)$,

$$S_1(Q,\omega)=S_{\mathrm{PR}}(Q,\omega)+S_{\mathrm{L}}(Q,\omega). \tag{4}$$

To obtain $S_1(Q,\omega)$, we must subtract the broad component $S_B(Q,\omega)$ from Eq. (1). $S_B(Q,\omega)$ is shown in Figs. 2 and 4 at two wave vectors and was found to be independent of filling

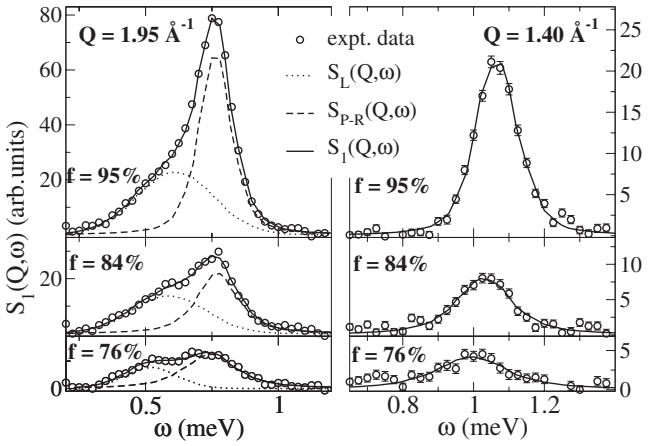

FIG. 5. Net observed $S(Q,\omega)$ at $T=0.4$ K with the broad component $S_B(Q,\omega)$ subtracted (points). The solid line is a best fit of the single mode $S_1(Q,\omega)$ given by Eq. (4). At $Q=1.40$ Å^{-1}, $S_1(Q,\omega)$ includes a P-R mode only with $S_{PR}(Q,\omega)$ given by Eq. (5). At $Q=1.95$ Å^{-1}, $S_1(Q,\omega)$ contains $S_{PR}(Q,\omega)$ plus a layer mode with $S_L(Q,\omega)$ given by Eq. (7).

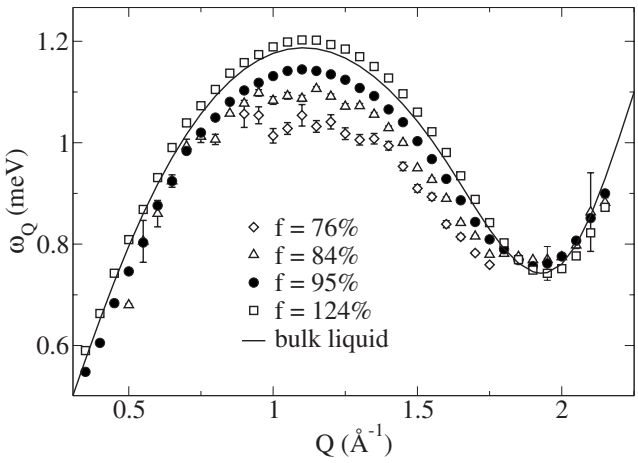

FIG. 6. Phonon-roton energies at $T=0.40$ K and several fillings. The solid line is the energies in bulk superfluid helium from Ref. 46.

for $f \gtrsim 76\%$. Similarly, at Q values other than the roton Q, the multiple scattering component $I_{MS}(Q,\omega)$ was subtracted from Eq. (1), as discussed above in Sec. III. $S_{PR}(Q,\omega;T)$ was represented by the usual damped harmonic oscillator function,[31,44]

$$S_{PR}(Q,\omega) = \frac{[n_B(\omega)+1]}{\pi}\left[\frac{\Gamma_Q}{(\omega-\omega_Q)^2+\Gamma_Q^2} - \frac{\Gamma_Q}{(\omega+\omega_Q)^2+\Gamma_Q^2}\right], \tag{5}$$

where ω_Q, Γ_Q, and Z_Q are free fitting parameters and

$$n_B(\omega) \equiv \frac{1}{e^{\beta\hbar\omega}-1} \tag{6}$$

is the Bose function. The layer mode was represented by a Gaussian function,

$$S_L(Q,\omega) = \frac{A_Q}{\sqrt{2\pi}\sigma_Q} e^{-(\omega-\mu_Q)^2/2\sigma_Q^2}, \tag{7}$$

where the energy μ_Q, width σ_Q, and weight A_Q are free fitting parameters. Layer modes are attributed to excitations propagating in the liquid layers close to the dead layers adsorbed on the media walls.[16,18] We observed layer modes in $S_1(Q,\omega)$ at wave vectors $Q \gtrsim 1.8$ Å^{-1} only. At $Q \leqslant 1.70$ Å^{-1}, there was no resolvable layer mode, only a P-R mode. The $S_1(Q,\omega)$ was convoluted with the instrument resolution function and fitted to the data. The number of free parameters is then 3 for $Q<1.80$ Å^{-1} (ω_Q, Γ_Q, and Z_Q) and 6 for $Q \geqslant 1.80$ Å^{-1} (ω_Q, Γ_Q, Z_Q, μ_Q, σ_Q, and A_Q). Some examples of data along with the best fit of Eqs. (5) and (7) are shown in Fig. 5. The layer mode appears as a broad intensity on the low energy side of the roton peak ($Q=1.95$ K). The fitted ω_Q, which represent the P-R mode energies when Γ_Q is reasonably small,[44] are shown in Fig. 6. At partial fillings, the P-R energies lie below the bulk values for wave vectors in the range $0.5 \leqslant Q \leqslant 1.7$ Å^{-1}, especially centered around the maxon wave vector ($Q \simeq 1.1$ Å^{-1}). As the filling is increased, the mode energies move toward the bulk superfluid values. In other porous media investigated,[18,23,36,43,45] the mode energies were found to coincide with the bulk values at full filling ($f=100\%$) within precision. This appears to be the case in the present gelsil as well but is not unambiguously established since we did not investigate $f=100\%$ exactly. The intensity in the P-R mode also increases markedly with filling.

P-R mode energies that lie below the bulk values near the maxon Q are observed in superfluid ^{4}He films of three to five liquid layer thickness on graphite surfaces.[28,29] They are also observed in other media partially filled.[18–21,23] In aerogel, the roton energy was found[18] to lie above the bulk value at partial fillings and reduced to the bulk value at full filling. These differences from bulk energies suggest that the liquid density near the liquid-vapor surface in films on both graphite and porous media walls is less than the bulk density.

The parameter Γ_Q, which represents the half width at half maximum (HWHM) of the P-R modes, is shown in Fig. 7 as a function of Q. Typical values of Γ_Q at $f=84\%$ are greater than or comparable to the HWHM of the instrument resolution (50 μeV). As filling increases, Γ_Q decreases significantly. In other porous media, we have found[18,19,22,23,36,45] that Γ_Q appears to go to zero at low temperature at full filling ($f=100\%$) within instrument precision. The present Γ_Q also appears to go to zero at full filling within precision ($\Gamma_Q \lesssim 10$ μeV). In addition, it is interesting to note that at $f=95\%$, the mode energies around the maxon region shown in Fig. 6 differ from the bulk SVP values by $\delta\omega \sim 30$ μeV. Thus, the observed width at $f=95\%$ could arise in part from the existence of different mode energies in different regions (different densities) of the porous media as some pores reach full filling before others. Figure 8 shows the integrated intensities of the 3D-like P-R mode, Eq. (5), and the layer mode, Eq. (7), as a function of filling, scaled so that the intensity is unity at $f=100\%$. The intensity averaged over the available

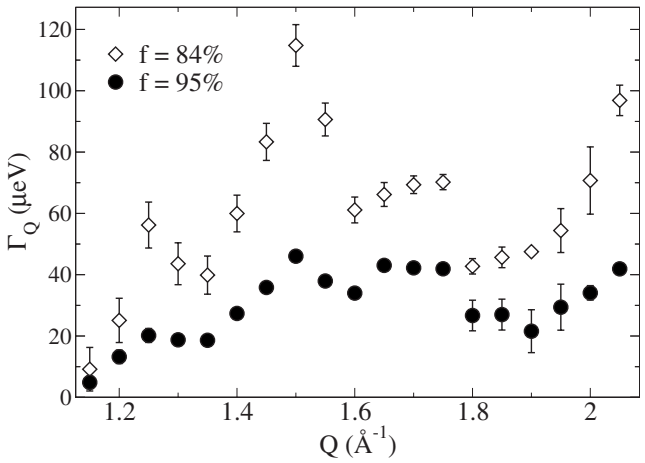

FIG. 7. The phonon-roton half width parameter Γ_Q of Eq. (5) at $T=0.4$ K as a function of Q at two fillings.

Q values is shown. The three vertical dashed lines indicate, from lower to higher filling, the completion of the multilayer, the completion of capillary condensation, and full filling, as identified in the adsorption isotherm, Fig. 1. In the filling range from the dead layer completion ($f=50\%$) to the start of the capillary condensation hysteresis loop ($f=84\%$), the layers denoted the multilayer are formed. In this range, there is also some filling of smaller pores by capillary condensation. The P-R (3D) and layer mode [two-dimensional (2D)] intensities begin in this filling range. Thereafter, the intensity in the P-R mode appears to increase approximately linearly with filling. The intensity in the layer mode is expected to saturate with filling eventually, but this range is not reached in this small pore media. Above $f=100\%$, we found, as expected, that the signal in the 2D mode does not increase significantly. All the additional scattering is found in the P-R mode. This signal comes from the helium condensed as bulk liquid between the porous sample and the sample holder. It is interesting that the rate of increase in the P-R mode intensity with filling is nearly the same at capillary condensation filling ($f=84\%$ to $f\approx 100\%$) as for the bulk (from $f=100\%$ to $f=124\%$).

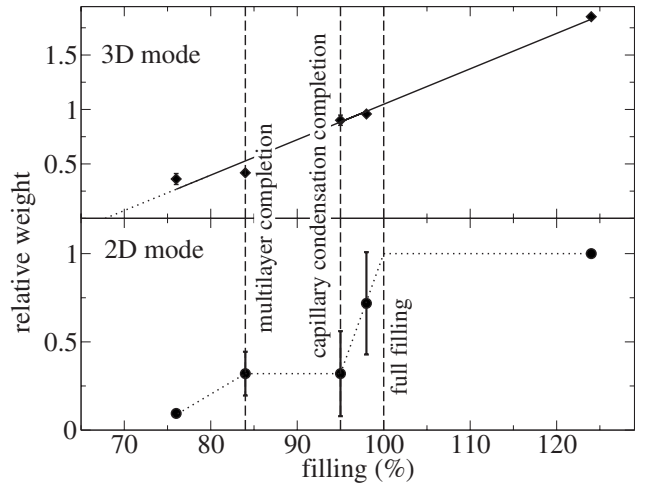

FIG. 8. The weight in the photon-roton mode (3D) and in the layer mode (2D) (averaged over the available Q values) vs filling assuming a weight of 1 at $f=100\%$ for each mode. The vertical dashed lines indicate the completion of filling processes, as obtained from the ^{4}He adsorption isotherm, Fig. 1.

C. Temperature dependence

The temperature dependence of the weight in P-R and layer modes was investigated at $f=95\%$ and temperatures of 1.35, 1.45, 1.60, 1.70, 1.80, 1.90, and 2.00 K. The lowest ($T=0.40$ K) and the highest ($T=2.25$ K) temperature data were used for reference only, as described below. With the multiple scattering subtracted, the following model was fitted to the data:

$$S(Q,\omega;T) = f_S(T)S_S(Q,\omega;T) + [1-f_S(T)]S_N(Q,\omega), \quad (8)$$

where

$$S_S(Q,\omega;T) = S_1(Q,\omega;T) + S_B(Q,\omega;T=0.4\text{ K}) \quad (9)$$

and $S_1(Q,\omega;T)$ is given by Eq. (4). $S_B(Q,\omega;T=0.4\text{ K})$ was obtained, as discussed above, by fitting Eq. (2) to the broad component at $T=0.4$ K. $S_N(Q,\omega)$ is the net observed intensity at high temperature, $T=2.25$ K, in the normal phase,

$$S_N(Q,\omega) = S(Q,\omega;T=2.25\text{ K}) = S_B(Q,\omega;T=2.25\text{ K}). \quad (10)$$

As seen from Figs. 2 and 3, $S_N(Q,\omega)$ is very broad. It is evident from Eqs. (8)–(10) that this formulation requires $f_S(T)$ to be 1 at $T=0.40$ K and zero at $T=2.25$ K. There is a broad component at both high and low temperatures. In the fitting process, the weights Z_Q and A_Q in the P-R and layer modes, respectively, were held constant at the value obtained above at $T=0.40$ K and $f=95\%$ independent of temperature. $\Gamma_Q(T)$ was set to the bulk superfluid values of Ref. 48 at each temperature to which we added the fitted value obtained here at $T=0.40$ K and $f=95\%$. The width of $S_L(Q,\omega)$ was assumed to be independent of temperature with σ_Q kept fixed at the value obtained at $T=0.40$ K and $f=95\%$. The fit then has two free parameters, ω_Q and $f_S(T)$ for $Q<1.80$ Å^{-1}, and three free parameters ω_Q, f_S, and the layer mode energy μ_Q of Eq. (7), for $Q\geqslant 1.80$ Å^{-1}. Examples of the fits are presented in Fig. 9.

The behavior of $f_S(T)$ is of great interest. It provides the weight of the single excitation component $S_1(Q,\omega;T)$ in $S(Q,\omega)$. A well-defined $S_1(Q,\omega;T)$ at higher wave vectors is a signature of BEC. The variation of $f_S(T)$ as a function of Q is shown in Fig. 10. We find that the parameter $f_S(T)$ is independent of Q over the range $1.25\leqslant Q\leqslant 2.10$ Å^{-1} and can be considered as temperature dependent only. The average of $f_S(T)$ over Q is shown in Fig. 11, together with the superfluid fraction, $\rho_s(T)$, for the bulk liquid. The $f_S(T)$ values for Vycor[23] are shown as an inset.

As in Vycor, we conclude that liquid helium in the present gelsil supports well-defined P-R modes at temperatures above the superfluid-normal transition temperature $T_c=1.92$ K. This suggests that there is BEC in the normal phase

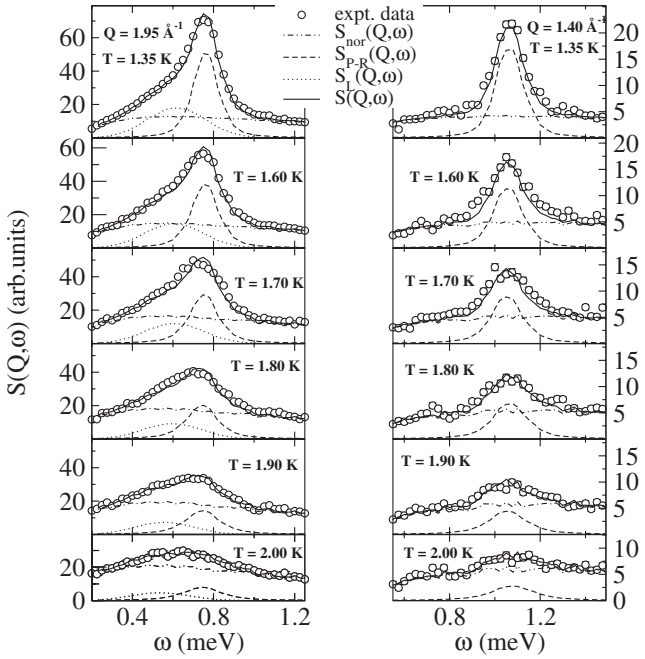

FIG. 9. Net observed $S(Q,\omega)$ (points) and best fit of $S(Q,\omega)$ of Eqs. (8), (9), and (4) to data to obtain $f_S(T)$ at the temperatures indicated. The symbol $S_{\rm nor}(Q,\omega)$ indicates the sum of the broad components: $S_{\rm nor}(Q,\omega)=f_S(T)S_B(Q,\omega;T=0.4\ {\rm K})+[1-f_S(T)]S_N(Q,\omega;T)$ given by Eqs. (8)–(10).

in the present porous media. Modes are observed up to a temperature $T\simeq 2.15$ K, slightly below T_λ. In Vycor,[23] where $T_c=2.05$ K, well-defined P-R modes were also observed above T_c, up to approximately T_λ. In the present gelsil, $T_c=1.92$ K lies further below $T_\lambda=2.17$ K than in Vycor, providing a clearer demonstration that there are well-defined P-R modes in the temperature range $T_c\leqslant T\leqslant T_\lambda$. The fraction of the P-R mode in $S(Q,\omega;T)$ in the present gelsil does not track the superfluid fraction of bulk liquid helium as was apparently the case for helium in Vycor.[23]

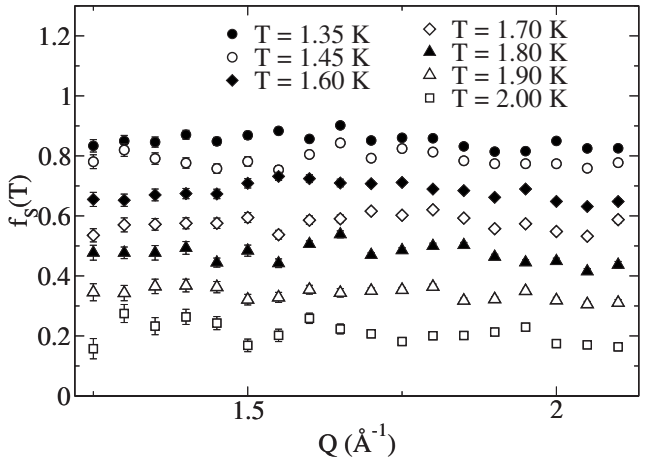

FIG. 10. Fraction $f_S(T)$ of the total $S(Q,\omega)$ taken up by the phonon-roton mode versus Q obtained by fits of Eq. (8) to data. An example fit at $Q=1.95$ Å^{-1} is shown in Fig. 9.

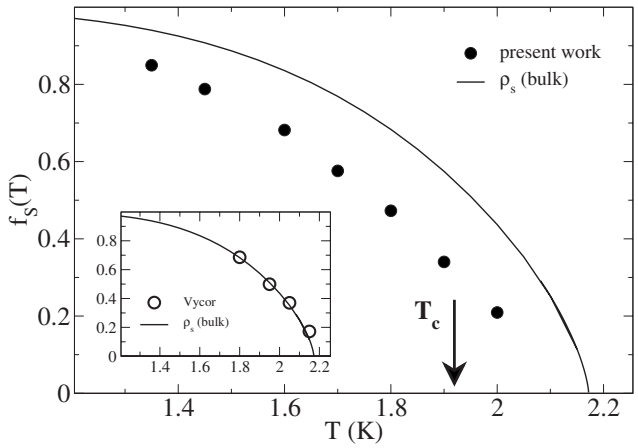

FIG. 11. Fraction $f_S(T)$ of the total $S(Q,\omega)$ taken up by the phonon-roton mode averaged over all P-R modes (all Q) versus temperature (solid circles). The arrow indicates the T_c for ^{4}He in the present gelsil. A finite $f_S(T)$ above T_c, and therefore a P-R mode above T_c, is indicated. Shown in the inset is $f_S(T)$ for ^{4}He in Vycor (Ref. 23) where $T_c=2.05$ K. The solid line shows the superfluid fraction of bulk liquid helium.

V. DISCUSSION AND CONCLUSIONS

A. Filling dependence

The present scattered intensity from ^{4}He in gelsil at partial fillings shows similarities with that from thin liquid ^{4}He films.[26–29] The structure and dynamics of films on graphitized carbon powder (graphon) and on an exfoliated and recompressed graphite (grafoil or payyex) have been extensively investigated.[20] On exfoliated graphite, the first two helium layers form 2D triangular lattices.[27] The third layer is liquid. Well-defined 3D-like P-R and layer modes are first observed when there are four layers deposited (two solid and two liquid layers). Thereafter, the intensity in the P-R mode increases linearly with filling. The intensity in the layer mode initially increases with filling but saturates to a constant value after ten layers (eight liquid) are deposited.[27] The layer mode propagates in the second to eighth liquid layers on the media walls. A ripplon is observed on the liquid film–vapor interface.[49]

In the present gelsil, which has an aerogel-like structure, the adsorption isotherm in Fig. 1 shows that 50% of the helium is tightly bound to the walls. The static structure factor $S(Q)$ of these tightly bound layers is characteristic of an amorphous solid (no Bragg peaks) having the same density as the subsequent liquid.[50] The first layer on aerogel is an amorphous solid.[51] These layers do not contribute inelastic scattering intensity in the energy range investigated here. A simple model of the pores, cylindrical pores with a Gaussian distribution of pore diameters centered at 44 Å, suggests that two layers are complete at 50%–55% filling. The subsequent layers are less tightly bound, probably liquid. The P-R mode is first observed at $f\simeq 76\%$ as the fourth layer (second liquid layer) is filling. The filling is clearly more complicated in gelsil with a distribution of pore sizes, puddling, and some capillary filling in crevices but the filling at which modes are

first observed is consistent with films. We also observe well-defined modes ($f \simeq 76\%$) before the onset of observable capillary filling ($f=84\%$) in the present gelsil. In MCM-41, P-R modes were observed only after the onset of capillary filling.[43] In MCM-41, which has smoother walls, we[22] observed ripplons on the liquid-vapor surface at partial filling. Ripplons have also been clearly observed on the surface of ^{4}He films on the interior of aerogel.[47] However, we did not observe ripplons in the present measurement. This may be because a significant coating of helium (a few solid or liquid layers) is required on a rough porous media to obtain a surface that is smooth enough to support ripplons). In the present gelsil, the pores are full (no liquid surface) after only approximately "five layers." Also, in the present gelsil, the intensity in the P-R mode and layer mode increases approximately linearly with filling (see Fig. 8). Again, since the present gelsil is full after approximately five layers (one to three liquid layers), we do not observe significant saturation of the layer mode intensity with filling.

The P-R energies in thin films on graphite (e.g., five liquid helium layers) are remarkably similar to those shown in Fig. 6 for partial fillings (e.g., $f=84\%$). The maxon energy at $Q \simeq 1.1$ Å^{-1} lies well below the bulk superfluid value in both cases (e.g., 0.1 meV at $f=84\%$ in gelsil and 0.06 meV in films). The roton energy lies slightly above the bulk value. A lower maxon energy suggests that the liquid density near a liquid-vapor surface is less than the bulk liquid density. This has been predicted for helium films[52] and for helium near the surface of liquid helium droplets.[53,54] The BE condensate fraction near a film surface is predicted[52] and observed[55] to be larger than the bulk value, suggesting a lower density. A roton energy (0.78 meV) that lies above the bulk value (0.742 meV) was also observed in partially filled (30%) aerogel,[18] consistent with a lower density near a film surface. In thick films and in fully filled porous media, the P-R mode energies coincide with bulk values.[20]

A complication in comparing maxon and roton energies versus filling is that a layer mode is included in the fit in the roton region but not in the maxon region. A layer mode at all Q is predicted,[29] but at lower Q, either its intensity is too small or it is unresolvable from the 3D P-R mode. In Fig. 5, the layer mode at the roton minimum ($Q=1.95$ Å^{-1}), denoted the layer roton, has an apparent energy of 0.52 meV at $f=76\%$ and 0.60 meV at $f=95\%$. The layer roton energy is 0.54 meV in films on graphite[20] and 0.55 meV in Vycor.[19,45] Krotscheck and Apaja[56] have calculated the layer roton energy and found that it depends on the areal density of the layers. A calculated value of 0.60 meV (6.9 K) is obtained at a layer density of 0.065 Å^{-2}. This is less dense than uniform bulk liquid helium at SVP, $\rho=0.0219$ Å^{-3} which has an areal density of 0.078 Å^{-2}. Krotscheck and Apaja emphasized that a layer mode differs from a strictly 2D mode since the layer mode propagates in several liquid layers adjacent to the media walls.

Albergamo *et al.*[22] have recently demonstrated that negative pressures can be created in liquid ^{4}He confined in MCM-41. This is created close to full filling (e.g., $97\% \lesssim f \lesssim 100\%$). For example, referring to the desorption isotherm in Fig. 1, one could begin at full filling, reduce the vapor pressure above the liquid somewhat, and move to the left along the "flat" top of the desorption isotherm. In this change, the pores remain fully filled with liquid and the liquid is stretched across the pore walls, establishing a metastable "negative" pressure and a lower liquid density. Negative pressures up to approximately −5.5 bar were created. At these negative pressures, the P-R peaks retain the same intensity and width as at full filling but the energy shifts in response to the negative pressure (e.g., the maxon energy reduces from 1.200 meV at SVP to 1.085 meV). Cavitation of the liquid or breaking of the liquid away from the walls limits the negative pressure to −5.5 bar. This negative pressure phenomenon which occurs near full filling is different from the filling dependence discussed here although metastable states during filling are also possible.

B. Temperature dependence

In bulk superfluid ^{4}He, the onset of Bose-Einstein condensation, well-defined P-R excitations, and superfluidity occur at the same temperature,[30–33] the normal-superfluid transition temperature T_λ. Specifically, superfluidity arises because there is BEC, because the phase of the condensate wave function $\Phi(r)$ is coherent and connected across the whole sample.[57,58] The superfluid velocity is the gradient of the phase, $v_s=(\frac{\hbar}{m})\nabla\Phi(r)$. Equally, well-defined phonon-roton excitations in the superfluid phase exist because there is BEC.[59–61] When there is a condensate, the density excitations (phonon-roton) and single quasiparticle excitations have the same energy.[59–61] There are therefore no quasiparticle excitations having energies below the P-R excitations to which the P-R excitations can decay. The P-R excitations can decay only to other P-R excitations, resulting in uniquely sharp excitations at low temperature.[62] This feature is lost at T_λ. The Landau theory of superfluidity relates superfluidity to the existence of well-defined P-R excitations.[63,64] Both have their origins in BEC.

In a porous media, the condensate can be localized by disorder.[7,19,22,36] That is, as temperature is lowered, the condensate forms first in favorable regions (e.g., in larger pores) at a temperature at or near T_λ. These initial islands of BEC are separated by regions of normal fluid. There is phase coherence within the islands only. As temperature is lowered further, the condensate fraction increases and the islands of BEC grow in size. At a critical temperature T_c, the islands are large enough and close enough together so that the phase between them is connected. Below T_c, there is a single phase in the BEC extended across the whole sample and macroscopic superfluid flow can be established. In this picture, the normal-superfluid transition T_c is associated with a localized-extended phase coherence crossover. We expect $T_c < T_\lambda$. This interpretation has analogies with the picture of the normal-superconducting transition in Josephson junction arrays, in disordered thin films, in the Mott insulator–superfluid transition in optical lattices, and in the much more complicated normal to superconducting transition in high T_c materials. In this interpretation, the P-R modes that we observe here at temperatures above T_c are supported in the islands of BEC that exist above T_c. Near T_c, the size of the islands is prob-

ably comparable to the pore size. The islands of BEC become smaller as temperature increases until they vanish at T_λ.

The superfluid density is typically measured both in bulk helium and in helium in porous media using a torsional oscillator technique.[1] To observe a superfluid density in the oscillator, superflow across the whole sample is required. The P-R modes and BEC are observed, as here, using neutron scattering. The neutrons, in contrast, are a local probe penetrating the sample and can observe P-R modes that exist in small, disconnected regions within the sample. Thus, to observe superflow, phase coherence across the whole sample is required while to observe P-R modes, phase coherence over short length scales only (e.g., a few nanometers) is required.

The P-R excitations of liquid ^{4}He at pressures from SVP up to 38.5 bars in the present gelsil sample have been observed recently.[24] For pressures up to 25 bars and $T=0.4$ K, the P-R modes are well defined and their energies agree with bulk values. However, above 26 bars, the P-R modes in the maxon and phonon regions ($Q \lesssim 1.5$ Å^{-1}) are not observed. Loss of modes in the maxon region can be readily understood[65] since the maxon energy at $p \geqslant 25$ bars exceeds twice the roton energy. The maxon therefore lies in the two excitation band and can decay into two rotons. The modes in the maxon region therefore broaden and disappear.[65] The apparent loss of modes at lower energy in the phonon region at $p > 26$ bars may simply be that the intensity in the phonon modes is too small to be observed at higher pressures. At $p \simeq 30-35$ bars, well-defined modes are observed only at wave vectors in the roton region, $Q \simeq 2.0$ Å^{-1}. At $p > 38.5$ bars and $T=0.4$ K, no P-R modes at all including the roton region were observed. Well-defined rotons were also not observed above $T=1.5$ K at $p=38.5$ bars, consistent with an extrapolation of T_λ to higher pressure.

Yamamoto *et al.*[66] reported a possible quantum phase transition (QPT) ($T \simeq 0$ K) from the superfluid to normal phase at pressure $p \simeq 35$ bars in 25 Å gelsil. It is interesting to speculate that this QPT may be related to loss of well-defined modes at higher presure. In a 34 Å mean pore diameter gelsil, we have recently observed[67] loss of all P-R modes at $p \geqslant 37$ bars and $T=0.4$ K. In turn, both loss of well-defined modes and a superfluid density may be related to loss of BEC. The condensate fraction is very small at high pressure.[68] With the present measurements and those of Pearce *et al.*[24,67], we have shown that we can determine the region of temperature and pressure where well-defined P-R modes exist in porous media. Equally, bulk liquid helium up to 160 bars and the possible existence of well-defined modes and superfluidity in helium at these pressures are exciting topics of current research.[69–72]

ACKNOWLEDGMENTS

The authors acknowledge the technical support from the ILL cryogenics laboratory. Partial support by the United States Department of Energy under research Grant No. DOE-FG02-03ER46038 is gratefully acknowledged.

[1] J. D. Reppy, J. Low Temp. Phys. **87**, 205 (1992).
[2] M. P. A. Fisher, P. B. Weichman, G. Grinstein, and D. S. Fisher, Phys. Rev. B **40**, 546 (1989).
[3] K. Huang, in *Bose Einstein Condensation*, edited by A. Griffin, D. W. Snoke, and S. Stringari (Cambridge University Press, Cambridge, 1995).
[4] M. Ma, P. Nisamaneephong, and L. Zhang, J. Low Temp. Phys. **93**, 957 (1993).
[5] G. E. Astrakharchik, J. Boronat, J. Casulleras, and S. Giorgini, Phys. Rev. A **66**, 023603 (2002).
[6] A. V. Lopatin and V. M. Vinokur, Phys. Rev. Lett. **88**, 235503 (2002).
[7] H. R. Glyde, F. Albergamo, R. T. Azuah, J. Bossy, and B. Fåk, Eur. Phys. J. E **12**, 63 (2003).
[8] H. R. Glyde, Eur. Phys. J. ST **141**, 75 (2007).
[9] E. W. Carlson, V. J. Emery, S. A. Kivelson, and D. Orgad, in *The Physics of Conventional and Unconventional Superconductors*, edited by K. H. Bennemann and J. B. Ketterson (Springer-Verlag, 2002).
[10] N. Trivedi, A. Ghosal, and M. Randeria, Int. J. Mod. Phys. B **15**, 1347 (2001).
[11] N. Markovíc, C. Christiansen, A. M. Mack, W. H. Huber, and A. M. Goldman, Phys. Rev. B **60**, 4320 (1999).
[12] A. van Otterlo, K. H. Wagenblast, R. Fazio, and G. Schon, Phys. Rev. B **48**, 3316 (1993).
[13] U. C. Tauber and D. R. Nelson, Phys. Rep. **289**, 157 (1997).
[14] C. Fort, L. Fallani, V. Guarrera, J. E. Lye, M. Modugno, D. S. Wiersma, and M. Inguscio, Phys. Rev. Lett. **95**, 170410 (2005).
[15] G. Coddens, J. de Kinder, and R. Millet, J. Non-Cryst. Solids **188**, 41 (1995).
[16] R. M. Dimeo, P. E. Sokol, C. R. Anderson, W. G. Stirling, K. H. Andersen, and M. A. Adams, Phys. Rev. Lett. **81**, 5860 (1998).
[17] O. Plantevin, B. Fåk, H. R. Glyde, J. Bossy, and J. R. Beamish, Phys. Rev. B **57**, 10775 (1998).
[18] B. Fåk, O. Plantevin, H. R. Glyde, and N. Mulders, Phys. Rev. Lett. **85**, 3886 (2000).
[19] H. R. Glyde, O. Plantevin, B. Fåk, G. Coddens, P. S. Danielson, and H. Schober, Phys. Rev. Lett. **84**, 2646 (2000).
[20] B. Fåk and H. R. Glyde, in *Advances in Quantum Many-Body Theory*, edited by E. Krotscheck and J. Navarro (World Scientific, Singapore, 2002) Vol. 4.
[21] C. R. Anderson, K. H. Andersen, W. G. Stirling, P. E. Sokol, and R. M. Dimeo, Phys. Rev. B **65**, 174509 (2002).
[22] F. Albergamo, J. Bossy, P. Averbuch, H. Schober, and H. R. Glyde, Phys. Rev. Lett. **92**, 235301 (2004).
[23] F. Albergamo, H. R. Glyde, D. R. Daughton, N. Mulders, J. Bossy, and H. Schober, Phys. Rev. B **69**, 014514 (2004).
[24] J. V. Pearce, J. Bossy, H. Schober, H. R. Glyde, D. R. Daughton, and N. Mulders, Phys. Rev. Lett. **93**, 145303 (2004).
[25] D. R. Daughton, Master's thesis, University of Delaware, 2003.
[26] B. Lambert, D. Salin, J. Joffrin, and R. Scherm, J. Phys. (Paris), Lett. **38**, L377 (1977).

[27] W. Thomlinson, J. A. Tarvin, and L. Passell, Phys. Rev. Lett. **44**, 266 (1980).
[28] H. J. Lauter, H. Godfrin, and P. Leiderer, J. Low Temp. Phys. **87**, 425 (1992).
[29] B. E. Clements, H. Godfrin, E. Krotscheck, H. J. Lauter, P. Leiderer, V. Passiouk, and C. J. Tymczak, Phys. Rev. B **53**, 12242 (1996).
[30] H. R. Glyde, *Excitations in Liquid and Solid Helium* (Oxford University Press, Oxford, 1994).
[31] E. F. Talbot, H. R. Glyde, W. G. Stirling, and E. C. Svensson, Phys. Rev. B **38**, 11229 (1988).
[32] K. H. Andersen, W. G. Stirling, R. Scherm, A. Stunault, B. Fåk, H. Godfrin, and A.-J. Dianoux, J. Phys.: Condens. Matter **6**, 821 (1994).
[33] A. Griffin, *Excitations in a Bose Condensed Liquid* (Cambridge University Press, Cambridge, 1993).
[34] M. H. W. Chan, K. I. Blum, S. Q. Murphy, G. K. S. Wong, and J. D. Reppy, Phys. Rev. Lett. **61**, 1950 (1988).
[35] G. M. Zassenhaus and J. D. Reppy, Phys. Rev. Lett. **83**, 4800 (1999).
[36] O. Plantevin, H. R. Glyde, B. Fåk, J. Bossy, F. Albergamo, N. Mulders, and H. Schober, Phys. Rev. B **65**, 224505 (2002).
[37] Also referred to as Geltech since they were initially fabricated by the Geltech Co.
[38] 4F International Co., 3636 Northwest 68 Lane, Gainesville, FL 32653.
[39] E. P. Barrett, L. G. Joyner, and P. P. Halenda, J. Am. Chem. Soc. **73**, 373 (1951).
[40] S. Brunauer, P. H. Emmet, and E. Teller, J. Am. Chem. Soc. **60**, 309 (1938).
[41] F. Mezei, Phys. Rev. Lett. **44**, 1601 (1980).
[42] A. D. B. Woods and E. C. Svensson, Phys. Rev. Lett. **41**, 974 (1978).
[43] F. Albergamo, J. Bossy, H. R. Glyde, and A.-J. Dianoux, Phys. Rev. B **67**, 224506 (2003).
[44] B. Fåk and B. Dorner, Physica B **234-236**, 1107 (1997).
[45] O. Plantevin, B. Fåk, H. R. Glyde, N. Mulders, J. Bossy, G. Coddens, and H. Schober, Phys. Rev. B **63**, 224508 (2001).
[46] R. J. Donnelly, J. A. Donnelly, and R. N. Hills, J. Low Temp. Phys. **44**, 471 (1981).
[47] H. J. Lauter, I. V. Bogoyavlenskii, A. V. Puchkov, H. Godfrin, A. Skomorokhov, J. Klier, and P. Leiderer, Appl. Phys. A: Mater. Sci. Process. **74**, S1547 (2002).
[48] K. Bedell, D. Pines, and A. Zawadowski, Phys. Rev. B **29**, 102 (1984).
[49] H. J. Lauter, H. Godfrin, V. L. P. Frank, and P. Leiderer, Phys. Rev. Lett. **68**, 2484 (1992).
[50] J. Bossy (private communication).
[51] H. Godfrin, J. Klier, V. Lauter-Pasyuk, H. Lauter, and P. Leiderer, ILL Experimental Report No. 6-01-171, 1998 (unpublished).
[52] E. W. Draeger and D. M. Ceperley, Phys. Rev. Lett. **89**, 015301 (2002).
[53] D. S. Lewart, V. R. Pandharipande, and S. C. Pieper, Phys. Rev. B **37**, 4950 (1988).
[54] A. Griffin and S. Stringari, Phys. Rev. Lett. **76**, 259 (1996).
[55] J. V. Pearce, S. O. Diallo, H. R. Glyde, R. T. Azuah, T. Arnold, and J. Z. Larese, J. Phys.: Condens. Matter **16**, 4391 (2004).
[56] E. Krotscheck and V. Apaja, Eur. Phys. J. ST **141**, 83 (2007).
[57] G. Baym, *Mathematical Methods in Solid State and Superfluid Theory* (Oliver and Boyd, Edinburgh, 1969).
[58] P. Nozières and D. Pines, *Theory of Quantum Liquids* (Addison-Wesley, Redwood City, CA, 1990), Vol. II.
[59] N. Bogoliubov, J. Phys. (USSR) **11**, 23 (1947).
[60] N. Hugenholtz and D. Pines, Phys. Rev. **116**, 489 (1959).
[61] J. Gavoret and P. Nozières, Ann. Phys. (N.Y.) **28**, 349 (1964).
[62] L. D. Landau and I. M. Khalatnikov, Zh. Eksp. Teor. Fiz. **19**, 637 (1949).
[63] L. D. Landau, J. Phys. (USSR) **5**, 71 (1941).
[64] L. D. Landau, J. Phys. (USSR) **11**, 91 (1947).
[65] J. V. Pearce and H. R. Glyde, J. Low Temp. Phys. **138**, 37 (2005).
[66] K. Yamamoto, H. Nakashima, Y. Shibayama, and K. Shirahama, Phys. Rev. Lett. **93**, 075302 (2004).
[67] J. V. Pearce, J. Bossy, H. Schober, and H. R. Glyde, report (unpublished).
[68] S. Moroni and M. Boninsegni, J. Low Temp. Phys. **136**, 129 (2004).
[69] F. Werner, G. Beaume, A. Hobeika, S. Nascimbène, C. Herrmann, F. Caupin, and S. Balibar, J. Low Temp. Phys. **136**, 93 (2004).
[70] P. Nozières, J. Low Temp. Phys. **137**, 45 (2004); **141**, 91 (2006).
[71] L. Vranješ, J. Boronat, and J. Casulleras, J. Low Temp. Phys. **138**, 43 (2005).
[72] L. Vranješ, J. Boronat, J. Casulleras, and C. Cazorla, Phys. Rev. Lett. **95**, 145302 (2005).